

Synthesized Oxygen-Vacant TiO₂ Nanopowders with Thermal Plasma Torch Evaporation Condensation Process

C.-Y. Tsai, H.-C. Hsi and K.-S. Fan

Abstract—The objective of this research is to establish a novel process for preparing the oxygen-vacant titanium dioxide (TiO_{2-x}) nanoparticles with a clean surface, high purity, and controllable size and dimension. Samples were synthesized via the gas-phase evaporation condensation method with transferred DC plasma torch as the heating source. TiO_{2-x} nanopowders were fabricated using different ratios of Ar/He as the plasma gases. The formed TiO_{2-x} nanoparticle was characterized with TEM, EDS and XRD. Experimental results showed that increasing the He addition to Ar plasma gas elevated the plasma temperature. High plasma temperature can cause the tungsten cathode to melt, gasify, and dope into TiO₂ structure, which inhibited the size growth and the crystallinity of formed anatase. TiO_{2-x} nanoparticles with anatase phase and particle size at 5–10 nm can be developed at the Ar/He = 75/25. The oxygen vacancy turned the color of TiO₂ from white to yellow.

Index Terms—oxygen vacancy, titanium dioxide, thermal, transferred DC plasma torch.

I. INTRODUCTION

Titanium dioxide (TiO₂) has been used in numerous applications as a photocatalyst. The manufacturing process of TiO₂ strongly influences the purity and physical properties of resulting nanoparticles; these properties subsequently affect the characteristics of TiO₂ photocatalytic reactions. TiO₂ nanoparticles can be synthesized via solution and vapor synthesis methods, such as sol-gel [1]–[3], thermal hydrolysis [4], hydrothermal processing [5], chemical vapor deposition [6] and evaporation condensation [7], [8].

Evaporation condensation has shown to possess advantages to develop nanoparticles and film with clean surface and a narrow particle size distribution. The heating sources for evaporation condensation include electron beam, laser and plasma [8]–[10]. Plasma has been referred to as an economic heating source and can provide sufficient energy to directly vaporize TiO₂ precursors. Cold plasma such as microwave [11] was successfully used to prepare TiO₂ photocatalyst. However, because the temperature of cold plasma was generally around room temperature, gaseous

precursors were required for processing. Theoretically, TiO₂ nanoparticles with a high purity can be obtained by a direct combination of titanium atom and oxygen. The high melting point of titanium metal (i.e., 1941 K) makes the direct combination difficult to process. The sufficient energy provided by thermal plasma can vaporize metals with high melting points and makes the direct combination process possible [12].

Oxygen-deficient TiO₂ (TiO_{2-x}) has been extensively studied due to its photocatalytic properties under a visible light (VL) environment. Nakamura *et al.* prepared TiO_{2-x} for NO removal. A ST-01 sample (Ishihara Sangyo Kaisha, 100% anatase) was treated with radio-frequency discharge using a reducing gas (H₂) as the plasma gas. The authors concluded that the appearance of the VL activity was attributed to the newly formed oxygen vacancy state between the valence and the conduction bands in the TiO₂ band structure [13]. Ihara *et al.* manufactured TiO_{2-x} by calcinating the hydrolysis products of Ti(SO₄)₂ with NH₃ in an ordinary electric furnace in dry air at 400 °C [14].

TiO_{2-x} was generally developed by further modifying available TiO₂ via reduction reactions or thermal treatments, thus a multiple step synthetic process was needed. Few studies were shown to produce TiO_{2-x} in a single step. This study aimed at preparing TiO_{2-x} nanopowders by direct combination of vaporized Ti atoms with oxygen. A single-step evaporation condensation was established using a transferred DC plasma torch as the heating source. The mixture of argon (Ar) and helium (He) was used as the plasma gas to achieve a high-temperature environment [15]. We considered this single-step process a potential method to produce high-quality nanoscale TiO_{2-x} with clean surface and a narrow particle size distribution.

II. EXPERIMENTAL

Fig. 1 shows the schema of experimental apparatus for preparing TiO_{2-x} nanoparticles using a thermal plasma torch. The system comprised a DC transferred plasma torch connected to a 5 kW DC power supply (Model PLA-250 A, Taiwan Plasma Corp., Taiwan), a water-cooled stainless steel reaction chamber, a stainless steel powder filter (Tee-Type Filters, Swagelok) and a vacuum pump for shifting the particle floated in the exhaust gas. The plasma torch consisted of a tungsten cathode, which was cooled in the central tunnel with water and in the suburbs with sheath gases (O₂). Titanium metal with 99.8% purity was used as the anode; TiO_{2-x} nanopowder was formed by the direct combination of evaporated titanium atoms from the anode target with oxygen gas (99.99% purity) within the thermal plasma environment. TiO_{2-x} was synthesized at various

C.-Y. Tsai is with the Department of Safety, Health and Environment Engineering, National Kaohsiung First University of Science and Technology, 1, University Rd., Kaohsiung 824, Taiwan (e-mail: u9315918@nkfust.edu.tw)

H.-C. Hsi is with the Institute of Environmental Engineering and Management, National Taipei University of Technology, 1, Sec. 3, Chung-hsiao E. Rd., Taipei 106, Taiwan (corresponding author; phone: +886-2-27712171ext4126; fax: +886-2-87732954; e-mail: hchsi@ntut.edu.tw)

K.-S. Fan is with the Department of Safety, Health and Environment Engineering, National Kaohsiung First University of Science and Technology, 1, University Rd., Kaohsiung 824, Taiwan (e-mail: ksfan@nkfust.edu.tw)

He/Ar volume ratio (0/100, 15/85, 25/75, and 50/50) as plasma gas (total flow rate of 2 L/min; from position A in Fig. 1), the operating current of 110 A has been evaluated to be the optimal applied current for nanopowder synthesis. O₂ was used as both the reacting gas and the shelter gas of plasma torch (2 L/min; from position B in Fig. 1). The tail gas containing the formed TiO_{2-x} nanoparticles was passed through a stainless steel powder filter and a buffer tank induced by a vacuum pump.

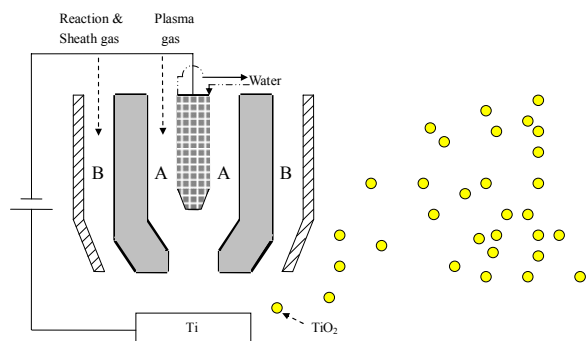


Fig. 1. Schematic diagram of transferred DC plasma torch for producing oxygen-vacant TiO₂ nanoparticles.

The formed TiO_{2-x} nanoparticles were collected using DI water from the stainless steel powder filter for sample characterization. A drop of suspension was dispersed in ethanol, placed onto a carbon-coated Cu grid followed by air-drying to remove the solvent, and then analyzed with a transmission electron microscope (TEM, Philips CM-200) to investigate samples' morphology and particle size. The purity of nanoparticles was identified using an energy dispersive X-ray analyzer (EDS, OXFORD, JEOL JEM-2100F) operated at 200 kV accelerating voltage. Nanoparticles which placed on silver membrane filter paper. Powder X-ray diffraction (XRD, Shimadzu XRD-6000) was used for crystal structure identification. The scan range 2θ was between 20 and 80° with a scanning rate of 0.02°/s.

III. RESULTS AND DISCUSSION

Fig. 2 shows the TEM images of nanopowders synthesized at a fixed current of 110 A with various ratios of He/Ar as the plasma gas. It was observed that the diameter of the nanoparticles was 5–10 nm with 100% Ar as the plasma gas. When the He/Ar ratio increased to 15/85, the size of formed nanopowders appeared to increase to 5–50 nm. The size of nanoparticles grew at a larger He/Ar ratio is attributed to the greater thermal conductivity of He (0.144 at 273 K) as compared to that of Ar (0.0173 at 273 K). Therefore, the plasma formed at He/Ar = 15/85 possessed a higher temperature that caused the growth of TiO₂ nuclei. If this proposed mechanism hold, TiO₂ nanoparticles with a much larger size should be observed as the He/Ar mixing ratio greater than 15/85. The particle sizes of formed TiO₂ at He/Ar = 25/75 and 50/50, however, were approximately 5–10 nm, indicating that the expected growth of TiO₂ nuclei at an evaluated He/Ar ratio greater than 15/85 was not observed. The observed phenomena may be resulted by an unwanted tungsten contamination in the formed TiO₂

nanoparticles at high plasma temperature. A more detailed discussion will be presented later in this paper.

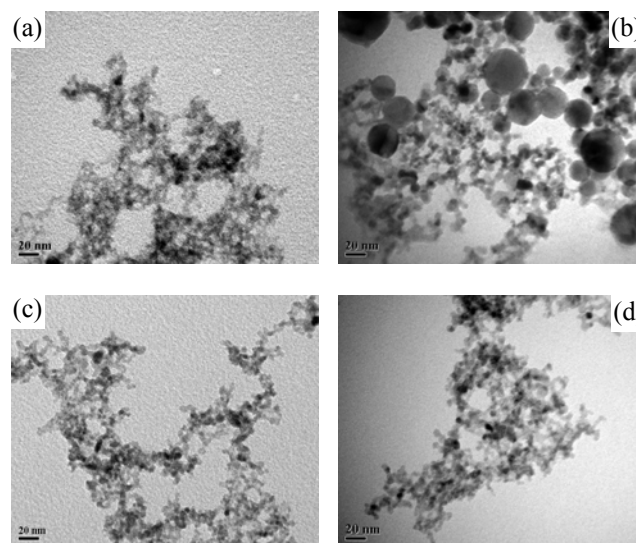


Fig. 2. TEM images of TiO_{2-x} powders synthesized at a 110 A plasma current and He/Ar ratio of (a) 0/100, (b) 15/85, (c) 25/75 and (d) 50/50.

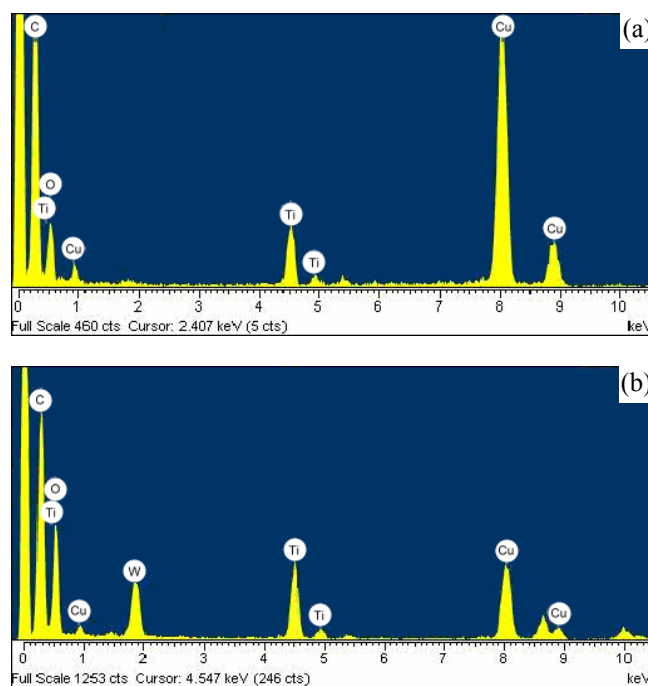


Fig. 3. EDS images of TiO₂ powders synthesized a 110 A plasma current and He/Ar ratio of (a) 0/100 and (b) 50/50.

The EDS results for TiO₂ prepared at a current of 110 A and 100/0 and 50/50 (Ar/He) plasma gases are shown in Fig. 3. The acquired results indicated that TiO₂ nanopowders with a very high degree of purity were developed under the 100/0 plasma gas condition. A small amount of W was observed to melt and subsequently gasify from the plasma cathode and doped into the TiO₂ nanopowders when 50% He was added to the plasma gas. Accompanying with the results obtained from the TEM analyses, it appeared that the gasified W doped into the formed TiO₂ may restrain particles growth [16]–[18]. Lee *et al.* prepared nano-sized Al-doped TiO₂ powders using a DC plasma jet as the heating source and

TiCl₄ and AlCl₃ as precursors. SEM results indicated that the size of particles decreased as increasing the amount of Al dopant [18]. The size reduction was attributed to the suppression of particle growth by Al species introduced into TiO₂ crystal [19]. This consequence can interpret the doped metal restraining the nanoparticles growth, which is consonant with the upshot of TEM shown in Fig. 2.

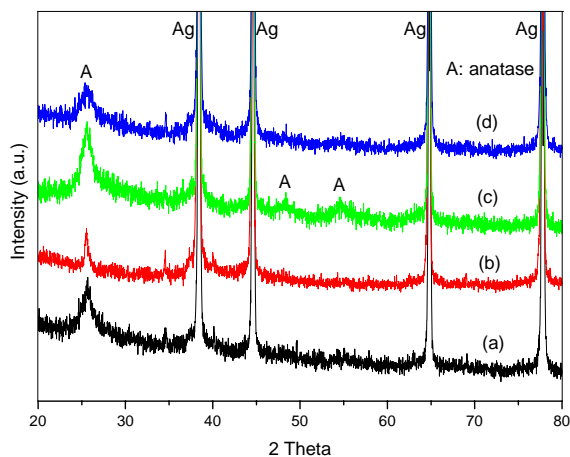


Fig. 4. XRD patterns of the nanopowders synthesized at the He/Ar ratio of (a) 0/100, (b) 15/85, (c) 25/75 and (d) 50/50.

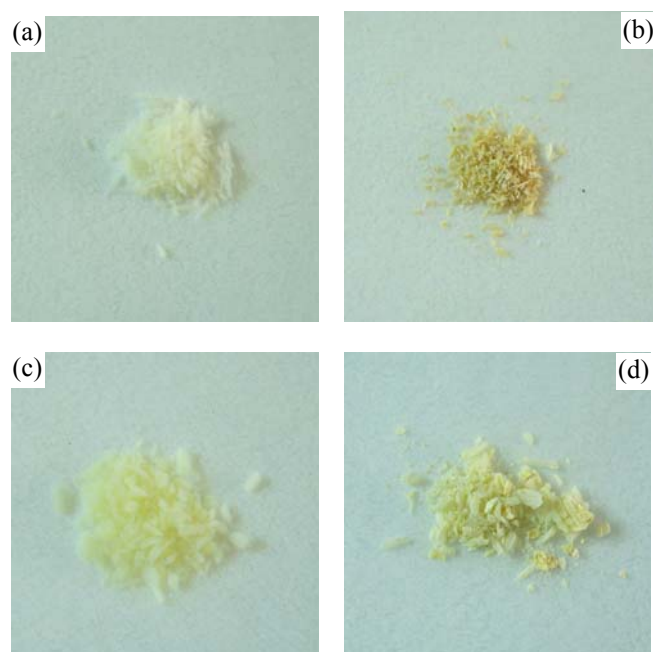


Fig. 5. Photographs of the nanopowders synthesized at the He/Ar ratio of (a) 0/100, (b) 15/85, (c) 25/75 and (d) 50/50.

Fig. 4 shows the XRD patterns of the TiO₂ nanopowders synthesized at different He/Ar ratios. Because the TiO_{2-x} nanopowders were laid on a silver membrane filter paper for XRD examination, four significant diffractive peaks contributed by Ag were shown. The XRD results clearly indicated that anatase was formed in the thermal plasma system, based on the observation of diffraction angle at $2\theta = 25.28^\circ$. These results also suggested that anatase TiO₂ with the greatest integrity of crystalline was obtained at the He/Ar ratio of 25/75. This result is expected because amorphous TiO₂ can transform into anatase or rutile as increasing

temperature, which is elevating by adding 25% He into the Ar plasma gas. Notably, the anatase peaks for the sample synthesized at the He/Ar ratio of 50/50 are less sharp as compared to those obtained at the He/Ar ratio of 25/75. It was suspected that the melted W doped into the formed TiO_{2-x}, causing defects in the crystal structure of anatase.

A number of literatures [13], [14], [20], [22] presented that the TiO₂ powder color changed from white to yellow due to oxygen vacancy in the crystal lattice of TiO₂. The photographs of TiO₂ nanopowders synthesized in the thermal plasma system showed that the color turned from white to yellow as increasing the He/Ar ratio (Fig. 5). Because the addition of He to Ar plasma gas elevated the plasma jet temperature, these observed results confirmed again that increasing the reaction temperature resulted in the oxygen vacancy of TiO₂.

IV. CONCLUSION

TiO_{2-x} nanoparticles was synthesized using a gas-phase evaporation condensation method with transferred plasma torch as the heating source. Results showed that TiO₂ nanopowders with a very high degree of purity can be developed using 100% Ar as the plasma gas. The characteristics of synthesized nanopowders markedly affected by the amount of He added to the plasma gas. When 15% He was added to Ar plasma gas, the nanoparticles size grew to 5–50 nm at a plasma current of 110 A. Oxygen-vacant TiO₂ (i.e., TiO_{2-x}) was formed as He was added to the Ar plasma gas, which increased the plasma temperature. The tungsten melted and gasified from the plasma cathode doped into the TiO₂ nanopowders, which influenced the crystal structures and powder size of formed TiO_{2-x}. XRD examination demonstrated that the single crystal of anatase was obtained at 110 A and 25% He/Ar ratio = 25/75. The oxygen vacancy in TiO₂ caused the color turning from white to yellow.

ACKNOWLEDGMENT

This work was supported by National Council of Taiwan (NSC94-2622-E-327-003-CC3) and Taiwan Plasma Corp., Kaohsiung, Taiwan.

REFERENCES

- [1] H. Yamashita, M. Harada, J. Misaka, M. Takeuchi, K. Ikeue, and M. Anpo, "Degradation of propanol diluted in water under visible light irradiation using metal ion-implanted titanium dioxide photocatalysts," *J. Photochem. Photobiol. (a)*, vol. 148, pp. 257-261, 2002.
- [2] S. P. Qiu, and S. J. Kalita, "Synthesis, processing and characterization of nanocrystalline titanium dioxide," *Mater. Sci. Eng. (a)*, vol. 435, pp. 327-332, 2006.
- [3] M. Kanna, and S. Wongnawa, "Mixed amorphous and nanocrystalline TiO₂ powders prepared by sol-gel method: Characterization and photocatalytic study," *Mater. Chem. Phys.*, vol. 110, pp. 166-175, 2008.
- [4] M. C. Hidalgo, and D. Bahnemann, "Highly photoactive supported TiO₂ prepared by thermal hydrolysis of TiOSO₄: Optimisation of the method and comparison with other synthetic routes," *Appl. Catal. (b)*, vol. 61, pp. 259-266, 2005.
- [5] X. H. Xia, Y. Liang, Z. Wang, J. Fan, Y. S. Luo, and Z. J. Jia, "Synthesis and photocatalytic properties of TiO₂ nanostructures," *Mater. Res. Bull.*, vol. 43, pp. 2187-2195, 2008.

- [6] X. W. Zhang, M. H. Zhou, and L. C. Lei, "Preparation of anatase TiO₂ supported on alumina by different metal organic chemical vapor deposition methods," *Appl. Catal. (a)*, vol. 282, pp. 285-293, 2005.
- [7] U. Backman, U. Tapper, and J. K. Jokiniemi, "An aerosol method to synthesize supported metal catalyst nanoparticles," *Synth. Met.*, vol. 142, pp. 169-176, 2004.
- [8] T. Sakai, Y. Kuniyoshi, W. Aoki, S. Ezoe, T. Endo, and Y. Hoshi, "High-rate deposition of photocatalytic TiO₂ films by oxygen plasma assist reactive evaporation method," *Thin Solid Films*, vol. 516, pp. 5860-5863, 2008.
- [9] Y. Suda, H. Kawasaki, T. Ueda, and T. Ohshima, "Preparation of high quality nitrogen doped TiO₂ thin film as a photocatalyst using a pulsed laser deposition method," *Thin Solid Films*, vol. 453-54, pp. 162-166, 2004.
- [10] S. H. Wang, T. K. Chen, K. K. Rao, and M. S. Wong, "Nanocolumnar titania thin films uniquely incorporated with carbon for visible light photocatalysis," *Appl. Catal. (b)*, vol. 76, pp. 328-334, 2007.
- [11] M. Addamo, M. Bellardita, D. Carriazo, A. Di Paola, S. Milioto, L. Palmisano, and V. Rives, "Inorganic gels as precursors of TiO₂ photocatalysts prepared by low temperature microwave or thermal treatment," *Appl. Catal. (b)*, vol. 84, pp. 742-748, 2008.
- [12] C. J. Liu, G. P. Vissokov, and B. W. L. Jang, "Catalyst preparation using plasma technologies," *Catal. Today*, vol. 72, pp. 173-184, 2002.
- [13] I. Nakamura, N. Negishi, S. Kutsuna, T. Ihara, S. Sugihara, and E. Takeuchi, "Role of oxygen vacancy in the plasma-treated TiO₂ photocatalyst with visible light activity for NO removal," *J. Mol. Catal. (a)*, vol. 161, pp. 205-212, 2000.
- [14] T. Ihara, M. Miyoshi, Y. Iriyama, O. Matsumoto, and S. Sugihara, "Visible-light-active titanium oxide photocatalyst realized by an oxygen-deficient structure and by nitrogen doping," *Appl. Catal. (b)*, vol. 42, pp. 403-409, 2003.
- [15] A. M. Fudolig, H. Nogami, J.-I. Yagi, K. Mimura, and M. Isshiki, "Prediction of surface temperature on metal beads subjected to argon-hydrogen transferred arc plasma impingement," *ISIJ*, vol. 37, pp. 623-629, 1997.
- [16] K.-N. P. Kumar, K. Keizer, and A. J. Burggraar, "Textural evolution and phase transformation in titania membranes: Part 1.—Unsupported membranes," *J. Mater. Chem.*, vol. 3, pp. 1141-1149, 1993.
- [17] B. Xia, H. Z. Huang, and Y. C. Xie, "Heat treatment on TiO₂ nanoparticles prepared by vapor-phase hydrolysis," *Mater. Sci. Eng. (b)*, vol. 57, pp. 150-154, 1999.
- [18] J. E. Lee, S. M. Oh, and D. W. Park, "Synthesis of nano-sized Al doped TiO₂ powders using thermal plasma," *Thin Solid Films*, vol. 457, pp. 230-234, 2004.
- [19] M. L. Taylor, G. E. Morris, and R. S. Smart, "Influence of aluminum doping on titania pigment structural and dispersion properties," *J. Colloid Interface Sci.*, vol. 262, pp. 81-88, 2003.
- [20] T. Sekiya, K. Ichimura, M. Igarashi, and S. Kurita, "Absorption spectra of anatase TiO₂ single crystals heat-treated under oxygen atmosphere," *J. Phys. Chem. Solids*, vol. 61, pp. 1237-1242, 2000.
- [21] T. Sekiya, S. Ohta, S. Kamei, M. Hanakawa, and S. Kurita, "Raman spectroscopy and phase transition of anatase TiO₂ under high pressure," *J. Phys. Chem. Solids*, vol. 62, pp. 717-721, 2001.
- [22] K. S. Rane, R. Mhalsiker, S. Yin, T. Sato, K. Cho, E. Dunbar, and P. Biswas, "Visible light-sensitive yellow TiO_{2-x}N_x and Fe-N co-doped Ti_{1-y}Fe_yO_{2-x}N_x anatase photocatalysts," *J. Solid State Chem.*, vol. 179, pp. 3033-3044, 2006.